Sensors and Materials, Vol. 36, No. 2 (2024) 671–681
MYU Tokyo

S & M 3554

Photoelectric Characteristics of Trilayer Thin-film Structures Processed at Different Annealing Temperatures for Photosensors

Tang-Yi Tsai,[1,2] Chia-Ju Liu,[1] Tsai-Dan Chang,[3]
Sheng-Lung Tu,[4] and Tao-Hsing Chen[3*]

[1]Graduate Institute of Science Education and Environmental Education, National Kaohsiung Normal University,
No. 116, Heping 1st Rd., Lingya District, Kaohsiung City 80201, Taiwan
[2]General Education Center, Open University of Kaohsiung,
No. 436, Daye North Rd., Siaogang Dist., Kaohsiung City, Taiwan
[3]Department of Mechanical Engineering, National Kaohsiung University of Science and Technology,
No. 415, Jiangong Rd., Sanmin Dist., Kaohsiung City 807618, Taiwan
[4]Department of Resources Engineering, National Cheng Kung University,
No. 1 University Road, Tainan City 70101, Taiwan

(Received June 20, 2023; accepted January 5, 2024)

Keywords: sputtering, transparent conducting film, annealing, ITO-doped Ga, Zr

Radio frequency (RF) magnetron sputtering was used to sputter a thin layer of ITO:Ga with a purity of 97:3 at% on glass substrates. A layer of Zr with a purity of 99.99% was then deposited on the ITO:Ga layer by direct current magnetron sputtering. Finally, RF magnetron sputtering was used once again to deposit a thin ZnO layer with a purity of 99.99 at% on top of the Zr layer. The three-layered film structure was annealed in a vacuum at various temperatures in the range of 200–500 °C in order to prompt a rearrangement of the crystal structure and reduce the number of internal defects. The effects of the annealing temperature on the film thickness, electrical properties, optical properties, surface morphologies, and quality factors of the multilayered films were investigated. The trilayer film showed a minimum resistivity of 1.79×10^{-3} Ω-cm after annealing at a temperature of 500 °C and an average optical transmission of 88.14% after annealing at 300 °C. The optimal quality factor (1.44×10^{-3} Ω^{-1}) was obtained for the film annealed at 500 °C.

1. Introduction

Transparent conducting oxide (TCO) films have good electrical conductivity and optical transparency, and are thus widely used in applications such as solar batteries, flat panel displays, thin-film transistors, and organic light-emitting components.[1–4] TCO technology dates as far back as 1902 with the discovery of CdO,[5] followed by the discovery of In_2O_3 (di-indium trioxide) some 50 years later. In more recent years, many TCO materials have been developed, including ZnO, SnO_2, and TiO_2.[6–9]

Furthermore, as micromachining technologies such as ion etching, reactive ion etching, ion injection, and magneton sputtering have advanced, the feasibility for

*Corresponding author: e-mail: thchen@nkust.edu.tw
https://doi.org/10.18494/SAM4684

ISSN 0914-4935 © MYU K.K.
https://myukk.org/

preparing TCO thin-film structures on suitable substrates has attracted growing attention. The literature contains many studies on the fabrication of TCO films using techniques such as molecular beam epitaxy,[10,11] metal-organic chemical vapor deposition,[12] radio frequency (RF) magnetron sputtering,[13–16] and pulsed laser deposition.[17] Most existing studies have been on the case of single TCO films on substrates. However, there is evidence to suggest that the electrical and optical properties of TCO films can be improved by developing multi-layered structures of carefully chosen TCO materials.

In this study, we utilize a magnetron sputtering system to fabricate trilayer TCO films consisting of ITO:Ga, Zr, and ZnO layers on glass substrates. The as-sputtered films are then annealed at temperatures in the range of 200–500 °C. The electrical and optical properties of the various films are systematically examined. The optimal coating is then selected as the coating that provides the best tradeoff between the electrical resistivity (lower is better) and optical transmittance (higher is better). The results show that the ITO:Ga/Zr/ZnO sandwich-structure film is suitable for the optical sensor and good optical sensor materials.

2. Methods

Corning gorilla glass plates were purchased from Fair & Cheer Incorporated Company and cut into small substrates of 25 × 25 × 7 mm^3 size using a diamond cutter. The substrates were washed sequentially in deionized (DI) water, acetone, and isopropanol, and then dried in an oven at 90 °C for 10 min to remove any moisture content. The sputtering process was performed using the parameters shown in Table 1 in a sputtering system. Note that for each layer, the sputtering parameters were assigned the values that optimized the tradeoff between the electrical properties and the optical properties of the respective single layer, as determined by preliminary experiments. The ITO:Ga target was purchased from Summit-Tech Resource Corp (Taiwan) and comprised In_2O_3:SnO_2 in a ratio of 90:10 wt% and a purity of 99.99% sintered with 3 at% Ga. In preparing the trilayer structure, the metal layer (Zr) was deliberately placed between the two oxide layers in order to minimize its oxidation during service, thereby affecting its electrical and optical properties. Following the sputtering process, the trilayer films were annealed in a vacuum for 5 min at temperatures of 200, 300, 400, and 500 °C in order to modify the film structure and change the electrical and optical properties accordingly.

The thickness of the trilayer films was measured under both the as-deposited condition and the annealed condition using an α-step profiler (KLA-Tencor). The crystalline structures of the films were examined using an X-ray diffractometer (XRD, SIEMENS D-500), whereas the optical properties were measured using a UV-VIS spectrometer (UV Solution 2900). The

Table 1
Deposition parameters for each layer in trilayer film.

Target category	Sputtering power (W)	Ar gas flow rate (sccm)	Working pressure (mTorr)	Sputtering duration (min)
ITO:Ga	80	15	6	30
Zr	20	15	10	1
ZnO	80	15	6	30

electrical properties of the films were measured using an AHM-800B 3141 Hall Effect Measurement System. Finally, the surface morphologies and surface roughness of the as-deposited and annealed films were observed by SEM (HITACHI SU-5000) and AFM (Bruker Dimension FastScan - XR), respectively.

3. Results and Discussion

3.1 Thickness and XRD property before and after film annealing

In this study, α-step was utilized to measure the film thickness, and the thickness of the trilayer film was 100.46 nm. Following the annealing process, the thickness varied by no more than ±2 nm among the various annealing conditions.

Figure 1 shows the XRD patterns of the as-deposited and annealed films. The patterns of the as-deposited film and film annealed at 200 °C show no prominent peaks and are thus inferred to have a noncrystalline structure. However, as the annealing temperature is increased to 300 °C, crystallization occurs. The peak intensities of the XRD patterns increase as the annealing temperature increases to 400 °C, but then decrease slightly at the highest annealing temperature of 500 °C. The present results are thus consistent with those of a previous study, in which the onset of ITO crystallization was found to occur at approximately 200 °C. Figure 1 shows that as the annealing temperature increases, the intensity of the main diffraction peak (222) increases sharply. In other words, the films annealed at 300 and 400 °C have a polycrystalline structure.

According to the literature, the ITO crystallization occurs at approximately 150–200 °C. With an annealing temperature of 200 °C, the crystallization appeared to be relatively slow and incomplete. With increasing annealing temperature, the main diffraction peak (222) increased significantly on the film surface; thus, the multilayer films annealed at 300 and 400 °C became

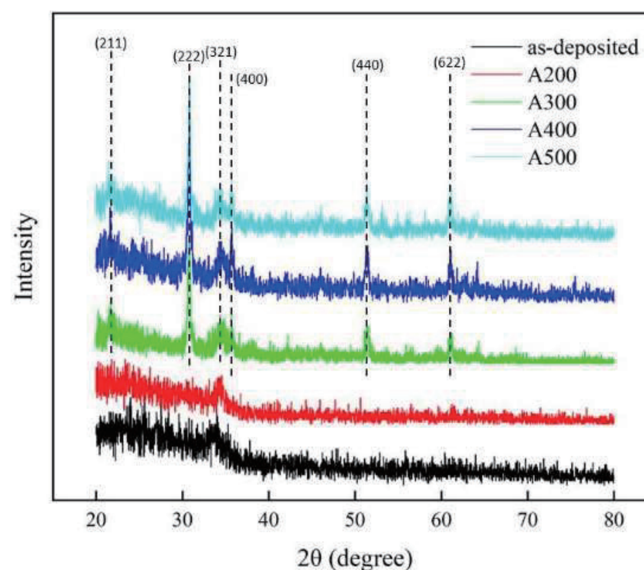

Fig. 1. (Color online) XRD patterns of ITO:Ga/Zr/ZnO trilayer films aged at different temperatures.

complete polycrystals. The manufactured ITO film with a sandwich structure (trilayer) contained a preferential (400) orientation. With RF magnetron sputtering, the manufactured film showed a preferred orientation on plane (440). As a result, the ITO layer after thorough annealing only presented a preferred (222) orientation since postdeposition annealing treatment of the sample can increase the intensity of the main diffraction peak of (222).

For the film annealed at 300 °C, diffraction peaks corresponding to the (211), (222), (321), (400), (440), and (622) planes were observed at 21.49°, 24.86°, 33.09°, 35.45°, 51.01°, and 60.65°, respectively. All of these peaks are consistent with those of In_2O_3. Thus, it is inferred that the Zr ions are fully incorporated into the In_2O_3 lattice owing to the effects of an elevated annealing temperature. It has been reported in previous studies that the incorporation of Zr into the ITO matrix improves the film density and reduces the gap size and number of defects between the grains.(18,19)

3.2 Electrical properties before and after annealing

The electrical performances of ITO:Ga/Zr/ZnO are shown in Fig. 2. A comparison of all the tested thin films reveals that high resistivity occurs in the as-deposited film. However, the resistivity decreases rapidly with increasing annealing temperature and has a minimum value of 1.79×10^{-3} Ω-cm after annealing at a temperature of 500 °C.

For the ITO:Ga/Zr/ZnO film, it was discovered from XRD results that both states after zero annealing and annealing at 200 °C were noncrystalline. Judging by the fact that internal grains of the film were still growing upon zero annealing and annealing at 200 °C, the peak value of In_2O_3 appeared when the annealing temperature was increased to 300 °C. After annealing at 300 °C, the grain rearrangement was complete and the resistivity started to increase, which was mainly caused by the change in carrier concentration.

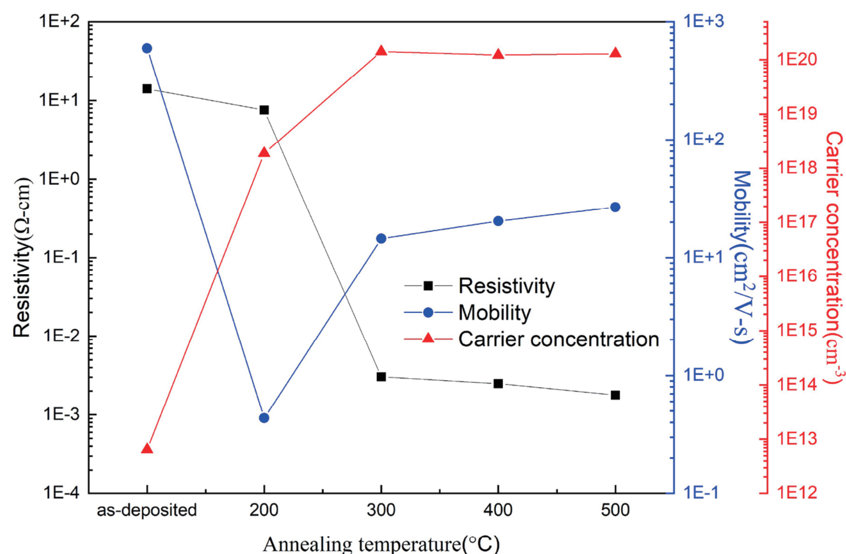

Fig. 2. (Color online) Electrical relationships of ITO:Ga/Zr/ZnO under different annealing temperatures.

3.3 Optical properties before and after annealing

From Table 2, the overall average transmittance of the trilayer film is shown as approximately 87–88%. It was also discovered that by increasing the annealing temperature, the optimal average transmittance of 88.14% could be achieved with the annealing temperature of 300 °C. The main reason was that the metal layer diffuses into the ITO thin film and ZnO thin film and then is replaced with oxides that enhance the transmittance. Overlapping the ZnO layer onto the Zr layer may cause a large scattering loss owing to the formation of a granular surface.

The optical energy gap values of the various ITO:Ga/Zr/ZnO trilayer films were calculated using the following Tauc plot equation.[20]

$$(ahv)^2 = A(hv - Eg) \tag{1}$$

Here, A is a constant, and α and hv represent the absorption coefficient and incident radiance, respectively. From the above formula, it was found that there is a linear relationship between $(ahv)^2$ and hv. Table 3 and Fig. 3 show that the energy gap was already 3.31 eV under the as-deposited condition, and the maximum energy gap of 3.56 eV was obtained after annealing at 500 °C. For average transmittance, the overall change was minimal, and the change in the energy gap was relatively small. However, the annealing temperature has only a minor effect on the energy gap value, and all of the energy gaps fall within the wide band gap (WBG) category of semiconductors.

Table 2
Optical properties of ITO:Ga/Zr/ZnO trilayer films annealed at different temperatures.

Transmittance average (%)	
Annealing temperature (°C)	ITO:Ga/Zr/ZnO
as-deposited	87.08
200	87.19
300	88.14
400	87.70
500	87.30

Table 3
Energy gap values of ITO:Ga/Zr/ZnO trilayer films annealed at different temperatures.

Energy gap (eV)	
Annealing temperature (°C)	ITO:Ga/Zr/ZnO
as-deposited	3.31
200	3.32
300	3.56
400	3.51
500	3.56

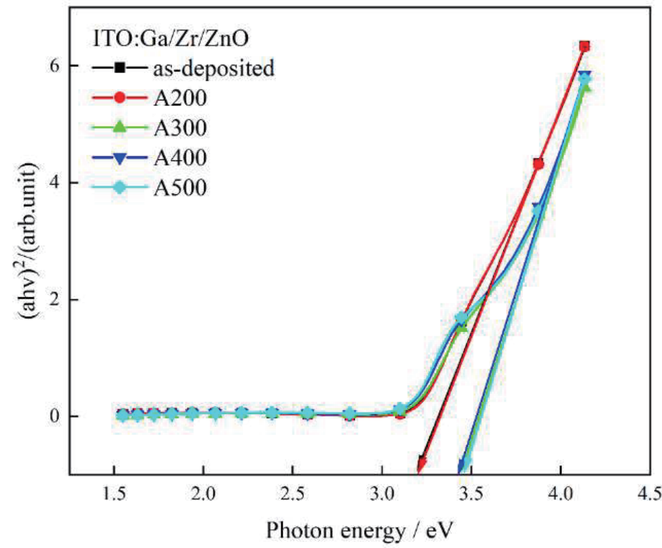

Fig. 3. (Color online) Energy gaps of ITO:Ga/Zr/ZnO under different annealing temperatures.

3.4 Surface feature analysis

The surface morphologies of the as-deposited and annealed ITO:Ga/Zr/ZnO trilayer films were observed by field-emission scanning electron microscopy (FE-SEM). The surface roughness profiles were analyzed by AFM, with the corresponding results quantified using the mean surface roughness (*Ra*). Figures 4(a)–4(e) show that when the annealing temperature is increased, the surface becomes smoother and the density increases. Figures 5(a)–5(e) are AFM images showing the surface conditions of different multilayer film structures. It can be observed in the figures that the deposited surface layers of both types of multilayer film structure have a dense texture. Table 4 presents the Ra values for ITO:Ga/Zr. All Ra values less than 1 nm indicate that the surface of the dual-layer film was very smooth. Furthermore, with the increase in annealing temperature, the Ra value increased. This means that the higher the annealing temperature, the higher the Ra value.

3.5 Grain size analysis

The grain sizes of the various coatings were calculated using the following Scherrer's formula:[21]

$$D = \frac{0.9\lambda}{\beta\cos\theta}, \quad (2)$$

where D is the grain size, λ is the X-ray incident angle of 0.15418 nm, θ is the angle of incident light, and β is the full width at half maximum (FWHM). Since the values for λ and θ were fixed while the reciprocal relation between D and β was known, the grain size would be larger when

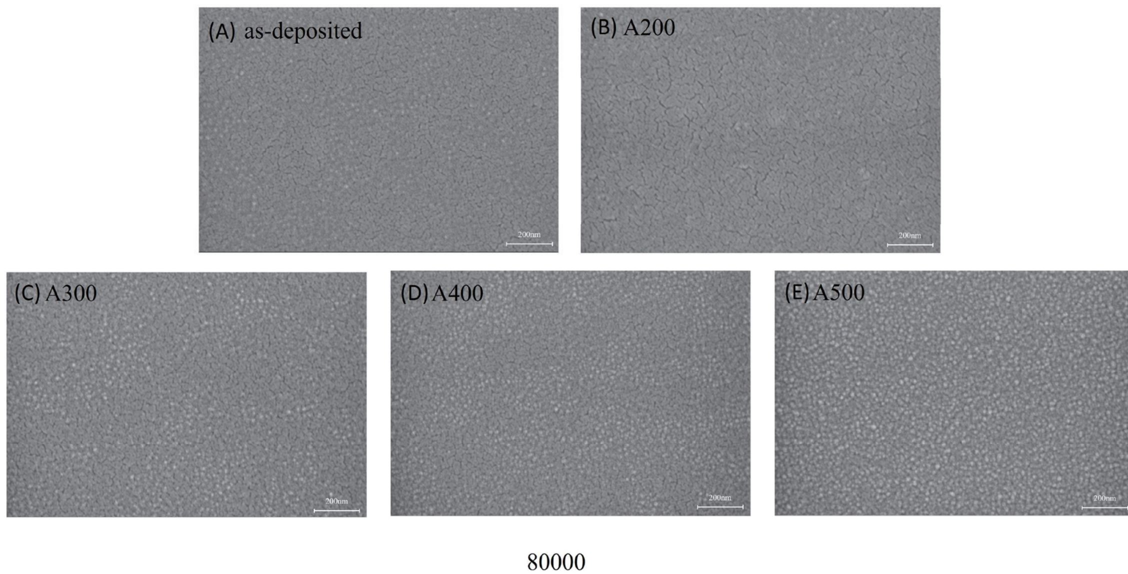

Fig. 4. ITO:Ga/Zr/ZnO multilayer thin films annealed at different temperatures: (a) as-deposited, (b) 200 °C, (c) 300 °C, (d) 400 °C, and (e) 500 °C.

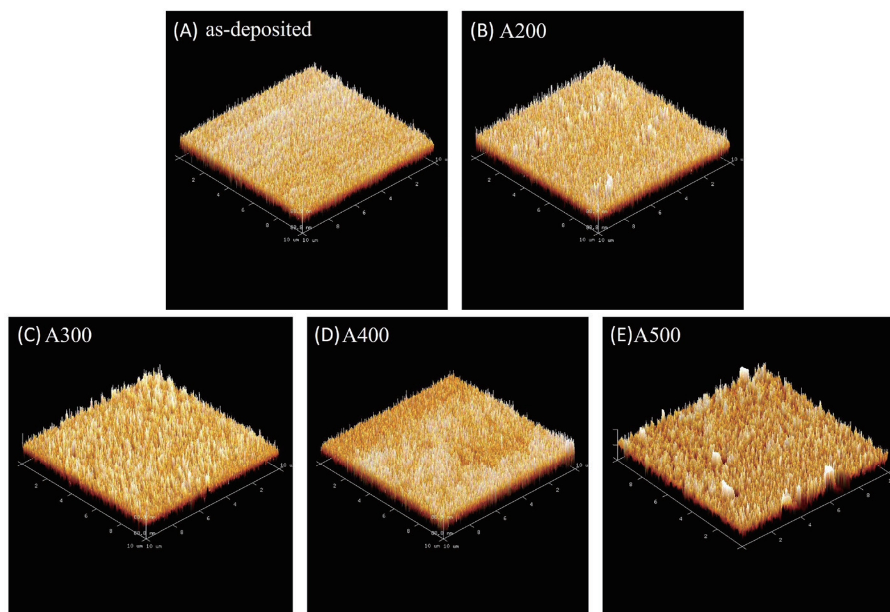

Fig. 5. (Color online) Three-dimensional AFM images of ITO:Ga/Zr/ZnO films annealed at different temperatures: (a) as-deposited, (b) 200 °C, (c) 300 °C, (d) 400 °C, and (e) 500 °C.

the FWHM is smaller. Figure 6 presents the FWHM and grain size relationships with the annealing temperature. It was observed from XRD that since there was no crystallization under the as-deposited condition and annealing at 200 °C, the grain size was not available. From the results, it was found that the grain size decreased and the FWHM increased with increasing annealing temperature.

Table 4
Mean surface roughness Ra of ITO:Ga/Zr/ZnO films annealed at different temperatures.

Ra (nm)	
Annealing temperature (°C)	ITO:Ga/Zr/ZnO
as-deposited	1.10
200	1.52
300	1.74
400	1.97
500	4.72

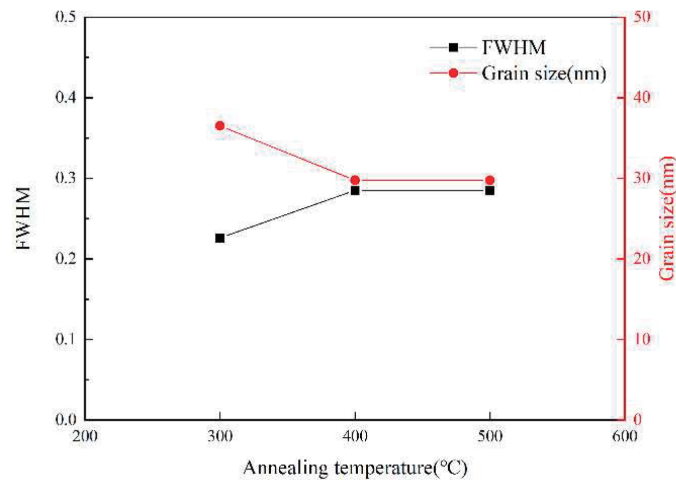

Fig. 6. (Color online) Effects of annealing temperature on FWHM and grain size of ITO:Ga/Zr/ZnO films.

3.6 Figure of merit (FOM) analysis

The quality of the ITO:Ga/Zr/ZnO films was evaluated using the following FOM:[22]

$$\Phi_{TC} = \frac{T_{av}^{10}}{R_{sh}}, \tag{3}$$

where T_{av} is the average optical penetration, R_{sh} is the film resistivity, and the unit is in Ω^{-1}. From the formula, it can be seen that the FOM is directly proportional to the penetration at a power of 10; thus, the penetration is found to affect the quality factor significantly. For a better FOM, higher penetration and lower resistivity values would be needed.

Table 5 and Fig. 7 show the FOM of ITO:Ga/Zr/ZnO. The optimal FOM was $1.44 \times 10^{-3}\ \Omega^{-1}$ when annealed at 500 °C, mainly because it possessed the lowest resistivity with a penetration of 87.30% after annealing, which made such a FOM the optimal value after comparison.

Table 5
FOM of ITO:Ga/Zr/ZnO with different annealing temperatures.

FOM Φ_{TC} (Ω^{-1})	
Annealing temperature (°C)	ITO:Ga/Zr/ZnO
as-deposited	1.56×10^{-9}
200	3.37×10^{-7}
300	9.37×10^{-4}
400	1.08×10^{-3}
500	1.44×10^{-3}

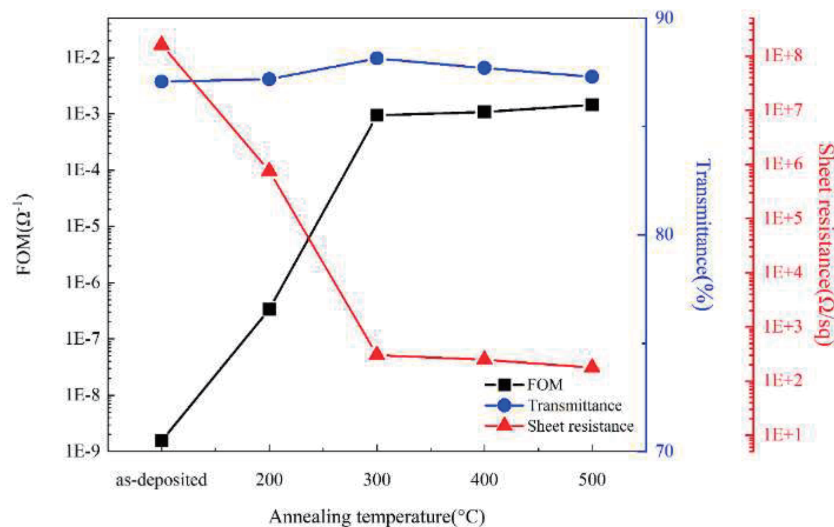

Fig. 7. (Color online) Analysis of quality factors of ITO:Ga/Zr/ZnO with different annealing temperatures.

4. Conclusions

We investigated the electrical and optical properties of trilayer ITO:Ga/Zr/ZnO films deposited on glass substrates using a magnetron sputtering system, followed by annealing at temperatures from 200 to 500 °C in a vacuum to obtain homogenous thin films.

The experimental results revealed that among the different annealing temperatures, the overall thicknesses of the ITO:Ga/Zr/ZnO films showed no significant differences after annealing. The XRD analysis results indicated that the ITO:Ga/Zr/ZnO film has a noncrystalline structure both under the as-deposited condition and after annealing at 200 °C. At annealing temperatures greater than 200 °C, however, a crystalline structure is formed, which consists mainly of In_2O_3 phases. The crystalline structure shows a strong (222) growth tendency and exhibits a maximum peak intensity in the film annealed at 400 °C. No clear Zr or ZnO peaks are observed in the annealed structures. The ITO:Ga/Zr/ZnO film annealed at 500 °C shows a minimum electrical resistivity of 1.79×10^{-3} Ω-cm, whereas that annealed at 300 °C shows the maximum average optical transmission of 88.14%. The maximum optical energy gap (3.56 eV)

occurs in the film annealed at 500 °C. The grain size decreases with increasing annealing temperature and has a value of 29.75 nm in the film annealed at 500 °C. The corresponding FWHM is 0.285. The film annealed at 500 °C shows the highest quality factor of $1.44 \times 10^{-3}\ \Omega^{-1}$ since it possesses the lowest resistivity and a high optical transmission for optical sensor applications.

Acknowledgments

This study is supported by Project Nos. MOST 110-2628-E-992-002 and 111-2628-E-992-001 MY2 of the Ministry of Science and Technology. The authors would like to thank the Ministry of Science and Technology for their support. The authors gratefully acknowledge the use of the XRD equipment of NSTC 111-2731-M-006-001 belonging to the Core Facility Center of National Cheng Kung University.

References

1 K. Kacha, F. Djeffal, H. Ferhati, L. Foughali, A. Bendjerad, A. Benhaya, and A. Saidi: Ceram. Int. **48** (2022) 20194. https://doi.org/10.1016/j.ceramint.2022.03.298
2 J. S. Jang, J. Kim, U. Ghorpade, H. H. Shin, M. G. Gang, S. D. Park, H.-J. Kim, D. S. Lee, and J. H. Kim: J. Alloys Compd. **793** (2019) 499. https://doi.org/10.1016/j.jallcom.2019.04.042
3 C. F. Liu, T. H. Chen, and J. T. Huang: Sens. Mater. **32** (2020) 3727. https://doi.org/10.18494/SAM.2020.3138
4 Y. Y. Jing, X. D. Tao, M. X. Yang, X. L. Chen, and C. Z. Lu: Chem. Eng. J. **413** (2021) 127418. https://doi.org/10.1016/j.cej.2020.127418
5 K. Badeker: Ann. Phys. **22** (1907) 749. https://doi.org/10.1002/andp.19073270409
6 J. H. Kim, T. Y. Seong, K. B. Chung, C. S. Moon, J. H. Noh, H.-J. Seok, and H.-K.Kim: J. Power Sources **418** (2019) 152. https://doi.org/10.1016/j.jpowsour.2019.02.018
7 T. H. Chen and C. L. Yang: Opt. Quantum Electron. **48** (2016) 533. https://doi.org/10.1007/s11082-016-0808-3
8 T. H. Chen and H. T. Su: Sens. Mater. **30** (2018) 2541. https://doi.org/10.18494/SAM.2018.2056
9 C. F. Liu, S. C. Shi, T. H. Chen, and G. L. Guo: Sens. Mater. **34** (2022) 4127. https://doi.org/10.18494/SAM4133
10 Z. X. Mei, Y. Wang, X. L. Du, Z. Q. Zeng, M. J. Ying, H. Zheng, J. F. Jia, Q. K. Xue, and Z. Zhang: J. Cryst. Growth **289** (2006) 686. https://doi.org/10.1016/j.jcrysgro.2005.12.086
11 H. C. Jang, K. Saito, Q. Guo, K. M. Yu, and T. Tanaka: J. Phys. Chem. Solids **163** (2022) 110571. https://doi.org/10.1016/j.jpcs.2021.110571
12 P. H. Lei and C. H. Cheng: Mater. Sci. Semicond. Process. **57** (2017) 220. https://doi.org/10.1016/j.mssp.2016.09.039
13 T. H. Chen, T. C. Cheng, and Z. R. Hu: Microsyst. Technol. **19** (2013) 1787. https://doi.org/10.1007/s00542-013-1837-5
14 T. H. Chen and T. Y. Chen: Nanomaterials **5** (2015) 1831. https://doi.org/10.3390/nano5041831
15 J. Wu, Z. Wang, F. Chen, Q. Shen, and L. Zhang: Appl. Surf. Sci. **493** (2019) 665. https://doi.org/10.1016/j.apsusc.2019.07.021
16 C. F. Liu, T. H. Chen, and Y. S. Huang: Sens. Mater. **32** (2021) 2321. https://doi.org/10.18494/SAM.2020.2867
17 R. S. Ajimsha, A. K. Das, P. Misra, M. P. Joshi, L. M. Kukreja, R. Kumar, T. K. Sharma, and S. M. Oak: J. Alloys Compd. **638** (2015) 55. https://doi.org/10.1016/j.jallcom.2015.02.162
18 G. K. Paul, S. Bandyopadhyay, S. K. Sen, and S. Sen: Mater. Phys. Chem. **79** (2003) 71. https://doi.org/10.1016/S0254-0584(02)00454-6
19 R. N. Chauhan and N. Tiwari: Thin Solid Films **717** (2021) 138471. https://doi.org/10.1016/j.tsf.2020.138471
20 T. Wang, Y. Liu, Q. Fang, M. Wu, X. Sun, and F. Lu: Appl. Surf. Sci. **257** (2011) 2341. https://doi.org/10.1016/j.apsusc.2010.09.100
21 M. Caglar, S. Ilican, and Y. Caglar: Thin Solid Films **517** (2009) 5023. https://doi.org/10.1016/j.tsf.2009.03.037
22 B. Sarma, D. Barman, and B. K. Sarma: Appl. Surf. Sci. **479** (2019) 786. https://doi.org/10.1016/j.apsusc.2019.02.146

About the Authors

Tang-Yi Tsai received his M.S. degree from the Graduate Institute of Science Education and Environmental Education, IEMBA, National Kaohsiung Normal University, Taiwan, in 2008. He is now a Ph.D. candidate of the Graduate Institute of Science Education and Environmental Education. His research interests are in environment engineering, environmental education, and environmental sensors. Furthermore, he is also an assistant professor in the General Education Center, Open University of Kaohsiung.
(vida.king@msa.hinet.net)

Chia-Ju Liu received her Ph.D. degree from the Graduate Institute of Science Education, National Taiwan Normal University, Taiwan, in 1999. She is now a professor at the Graduate Institute of Science Education and Environment, National Kaohsiung Normal University. Her research interests are in science education and optical sensors. (chiaju.nknu@gmail.com)

Tsai-Dan Chang received her B.S. degree from National Kaohsiung University of Science and Technology, Taiwan, where she is currently studying for her M.S. degree. Her research interests are in TCO thin films, materials engineering, and sensors.

Sheng-Lung Tu received his M.S. degree from the Department of Mechanical Engineering, National Cheng Kung University, in 2010 and his Ph.D. degree from the Department of Resources Engineering, National Cheng Kung University, in 2014. Since 2014, he has been working as a general affairs officer at National Cheng Kung University. His research interests are in PVD technology, thin-film technology, and sensors.

Tao-Hsing Chen received his B.S. degree from National Cheng Kung University, Taiwan, in 1999 and his M.S. and Ph.D. degrees from the Department of Mechanical Engineering, National Cheng Kung University, in 2001 and 2008, respectively. From August 2008 to July 2010, he was a postdoctoral researcher at the Center for Micro/Nano Science and Technology, National Cheng Kung University. In August 2010, he became an assistant professor at National Kaohsiung University of Applied Sciences (renamed National Kaohsiung University of Science and Technology), Taiwan. Since 2016, he has been a professor at National Kaohsiung University of Science and Technology. His research interests are in metal materials, TCO thin films, thermal sensors, and photosensors. (thchen@nkust.edu.tw)